

NUMERICAL EXPERIMENTS FOR SEGMENTING MEDICAL IMAGES USING LEVEL SETS

A. ARAÚJO, D. M. G. COMISSIÃO AND G. STADLER

ABSTRACT: Image segmentation is the process by which objects are separated from background information. Structural segmentation from 2D and 3D images is an important step in the analysis of medical image data. In this technical report, we utilize level set algorithms and active contours without edges to segment two and three-dimensional image data. Besides synthetical data, we also use magnetic resonance images of the human brain provided by the Institute of Biomedical Research in Light and Images of the University of Coimbra (IBILI).

KEYWORDS: Image segmentation, active contours, level sets, magnetic resonance images.

1. Introduction

Image segmentation refers to the process of separating objects in images from background information. Among others, it is of great interest for medical practitioners, for example for surgery planning or tumor treatment. In this context, often magnetic resonance (MR), computer tomography (CT), positron emission tomography (PET) or single photon emission computed tomography (SPECT) images are used.

When segmenting a medical image, the actual surfaces of identified objects are often blurred as a result of background noise generated by signal interference with surrounding tissues. Thus, efficient computational segmentation algorithms are required to accurately detect the outline of the regions of interest.

The level set method for capturing moving fronts was introduced by Osher and Sethian in 1988 [OS88]. This Eulerian-type method utilizes a fixed mesh of grid points, and matches the evolving interface implicitly with the zero-level contour of a signed-distance function. The resulting initial value partial differential equation is essentially a Hamilton-Jacobi equation. It is then possible to utilize entropy-satisfying schemes developed for the numerical solution of hyperbolic conservation laws.

Received November 6, 2006.

The success of level set methods is due to their efficiency and flexibility to deal with geometrical objects such as free boundaries and surfaces. Among its advantages, we mention the following: (i) Curvatures and normals are easily evaluated; (ii) Topological changes occur naturally; (iii) The technique is easily extended to three (or even more) dimensions. Moreover, level set theory is to a large amount based on the theory of partial differential equations (PDEs) and benefits from many of the results and techniques developed for such systems. A good introduction to the level set method and its use in image segmentation can be found in the texts by Osher and Fedkiw [OF03] and Sethian [Set99].

In this work we explain the basic ideas behind level set-based image segmentation and report on some numerical tests for both 2D and 3D data. To date, there is no universally accepted segmentation technique that works for all images. For our purposes, we have chosen to use active contour methods without edges.

2. Active Contours

The main idea behind algorithms for detecting active contours in image segmentation is easily explained. The user provides an initial guess for the contour. This guess is subsequently moved by image-driven forces to the boundaries of the desired objects. In such models, internal and external forces are considered. The internal forces defined within the curve are designed to keep the model smooth during the deformation process. External forces computed from the underlying image data are defined to move the model toward an object boundary or other desired features within the image.

2.1. The classical models. Let Ω be a bounded open set of \mathbb{R}^2 , with $\partial\Omega$ its boundary. Let $u_0 : \overline{\Omega} \rightarrow \mathbb{R}$ be a given image and $C : [0, 1] \rightarrow \mathbb{R}^2$ be a parameterized curve.

The main method used here is, that the curve C is evolved towards the object boundary under a force, until it stops at the boundary. To stop the process, an edge-detector is used, depending on the gradient of u_0 .

In the so-called snake model, we intend to find C^* such that $E(C^*) = \inf_C E(C)$, where

$$E(C) = \int_0^1 (\alpha |C'(s)|^2 + \beta |C''(s)|^2 - \lambda |\nabla u_0(C(s))|^2) ds, \quad \alpha, \beta, \lambda \in \mathbb{R}^+.$$

The first two terms of the energy functional $E(C)$ control the smoothness of the curve and the third one intends to attract the curve to the object boundary, where the image gradients are large. By minimizing the energy in this way, we are trying to locate the curve at the points of maximal $|\nabla u_0|$ (thus providing an edge-detector) while maintaining the smoothness of the evolving curve.

An edge-detector is a positive decreasing function g , depending on ∇u_0 , such that $\lim_{z \rightarrow 0} g(z) = 0$. One possible choice is

$$g(\nabla u_0(x, y)) = \frac{1}{1 + |\nabla G_\sigma(x, y) \star u_0(x, y)|^p} \quad \text{with } p \geq 1, \quad (1)$$

where $G_\sigma \star u_0$ is a smoother version of u_0 . For example, one can use the convolution of the image u_0 with G_σ , a Gaussian of variance σ . Note that $g(\nabla u_0)$ is positive and approximately one in homogeneous regions, and close to zero near the edges.

The use of the level set method, and in particular the motion by mean curvature of Osher and Sethian [OS88] is in this context specially justified due to its ability to naturally execute topological changes. With this method, the curve is represented implicitly via a Lipschitz function ϕ by the zero level set

$$C = \{(x, y) : \phi(x, y) = 0\},$$

and the evolution of C is given by the zero-level curve at time t of the function $\phi(x, y, t)$.

If we want the curve C to evolve in normal direction with speed a , we need to solve the partial differential equation

$$\frac{\partial \phi}{\partial t} = a|\nabla \phi|, \quad \phi(x, y, 0) = \phi_0(x, y)$$

with suitable boundary conditions. Here, the initial contour is given by the points (x, y) that satisfy $\phi_0(x, y) = 0$. Using motion by mean curvature, we have $a = k$, where k is the curvature of the level curve passing through (x, y) , i.e.,

$$k = \operatorname{div} \left(\frac{\nabla \phi(x, y)}{|\nabla \phi(x, y)|} \right).$$

A geometric active contour model based on the mean curvature motion is given by [CCCD93]

$$\begin{cases} \frac{\partial \phi}{\partial t} = g(\nabla u_0) |\nabla \phi| (k + \eta), & t \in \mathbb{R}^+, (x, y) \in \mathbb{R}^2, \\ \phi(x, y, 0) = \phi_0(x, y), & (x, y) \in \mathbb{R}^2, \end{cases}$$

where $g(\nabla u_0)$ is the edge function (1) with $p = 2$, η is a non-negative constant and ϕ_0 is the initial level set function. The zero level set curve moves in normal direction with speed $g(\nabla u_0)(k + \eta)$ and stops at the desired boundary, where g vanishes. The constant η is a correction term such that $k + \eta$ remains positive. In this case, η is a force pushing the curve towards the object, when $k \leq 0$. Also, $\eta \geq 0$ is a constraint on the area inside the curve, increasing the speed of propagation.

Another approach is the variational formulation of Zhao et al. [ZCMO96]

$$\frac{\partial \phi}{\partial t} = |\nabla \phi| g(\nabla u_0) k + \nabla g(\nabla u_0)^T \nabla \phi.$$

The first term corresponds to the motion in normal direction with velocity $g(\nabla u_0)k$ and the second one is a convective term in the direction of $\nabla g(\nabla u_0)$. Note that, if $g(\nabla u_0)$ vanishes, motion in normal direction stops and for constant $g(\nabla u_0)$, the convection term vanishes.

In practice, the edge-detector is never zero on the edges and therefore the evolving curve may not stop after having reached the desired contour. In [CV01], Chan and Vese propose a different active contour model without edges by using an edge-detector function that depends on the gradient ∇u_0 . The stopping term is based on the so-called Mumford-Shah segmentation technique.

2.2. Active contours without edges. Let us consider an open subset $\omega \subset \Omega$, such that $C = \partial\omega$. We will use the notation $\text{inside}(C) := \omega$ and $\text{outside}(C) := \Omega \setminus \omega$. Assume that the image u_0 is formed by two regions of approximately piecewise-constant intensities of distinct values u_0^i (the object to be detected) and u_0^o . Let us denote by C_0 the boundary of u_0^i . Then we have

$$u_0 \approx \begin{cases} u_0^i, & \text{inside}(C_0), \\ u_0^o, & \text{outside}(C_0). \end{cases}$$

Let us now consider the following “fitting term”

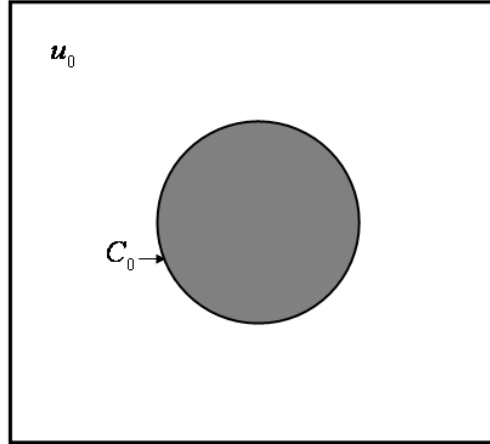


FIGURE 1. Test image.

$$F_1(C) + F_2(C) = \int_{\text{inside}(C)} |u_0(x, y) - c_1|^2 dx dy + \int_{\text{outside}(C)} |u_0(x, y) - c_2|^2 dx dy,$$

where C is any curve and c_1, c_2 depend on C and are the averages of u_0 inside C and outside C , respectively. Obviously, C_0 – boundary of the object – is the minimizer of the fitting term, i.e.,

$$\inf_C (F_1(C) + F_2(C)) \approx 0 \approx F_1(C_0) + F_2(C_0).$$

In fact (see Figure 2), if C is: outside the object, then $F_1(C) > 0$ and $F_2(C) \approx 0$; inside the object, then $F_1(C) \approx 0$ and $F_2(C) > 0$; both inside and outside the object, then $F_1(C) > 0$ and $F_2(C) > 0$; on the boundary of the object, then $F_1(C) \approx 0$ and $F_2(C) \approx 0$.

Our goal is to minimize the above fitting term plus some regularizing terms such as the length of the curve C and/or the area of the region inside C . Let us introduce the energy functional $F(c_1, c_2, C)$, defined by

$$F(c_1, c_2, C) = \mu \text{Length}(C) + \eta \text{Area}(C) + \lambda_1 F_1(C) + \lambda_2 F_2(C), \quad (2)$$

where $\mu \geq 0, \eta \geq 0, \lambda_i > 0, i = 1, 2$, are fixed parameters. Then, we are interested in solving the minimization problem

$$\min_{c_1, c_2, C} F(c_1, c_2, C).$$

We now rewrite the original model (2) in the level set formulation. Let the evolving curve C be

$$C = \partial\omega = \{(x, y) \in \Omega : \phi(x, y) = 0\},$$

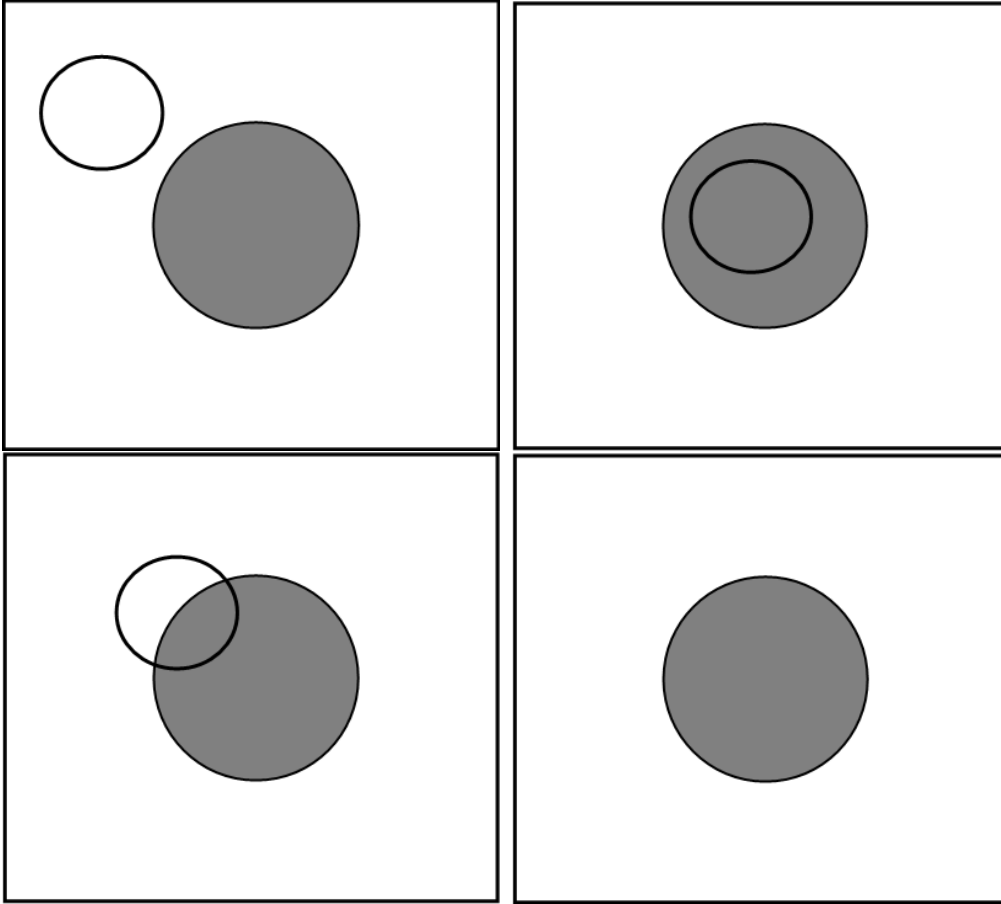


FIGURE 2. All possible cases in the position of the curve.

assuming that

$$\begin{cases} \text{inside}(C) = \omega = \{(x, y) \in \Omega : \phi(x, y) > 0\}, \\ \text{outside}(C) = \Omega \setminus \omega = \{(x, y) \in \Omega : \phi(x, y) < 0\}, \end{cases}$$

where $\omega \in \Omega$ is open.

For the level set formulation of our active contour model, we replace C by the unknown variable ϕ . Using the Heaviside function

$$H(z) = \begin{cases} 1, & \text{if } z \geq 0, \\ 0, & \text{if } z < 0, \end{cases}$$

and the Dirac delta function $\delta(z) = \frac{d}{dz}H(z)$ (in the sense of distributions), we can rewrite the energy functional in the following way:

$$\begin{aligned} \text{Length}(C) = \text{Length}(\phi = 0) &= \int_{\Omega} |\nabla H(\phi(x, y))| dx dy \\ &= \int_{\Omega} \delta_0(\phi(x, y)) |\nabla \phi(x, y)| dx dy; \end{aligned}$$

$$\text{Area}(C) = \text{Area}(\phi \geq 0) = \int_{\Omega} H(\phi(x, y)) dx dy;$$

$$F_1(C) = \int_{\phi > 0} |u_0(x, y) - c_1|^2 dx dy = \int_{\Omega} |u_0(x, y) - c_1|^2 H(\phi(x, y)) dx dy;$$

$$F_2(C) = \int_{\phi < 0} |u_0(x, y) - c_1|^2 dx dy = \int_{\Omega} |u_0(x, y) - c_1|^2 (1 - H(\phi(x, y))) dx dy.$$

Thus,

$$\begin{aligned} F(c_1, c_2, C) &= \mu \int_{\Omega} \delta_0(\phi(x, y)) |\nabla \phi(x, y)| dx dy + \eta \int_{\Omega} H(\phi(x, y)) dx dy \\ &\quad + \lambda_1 \int_{\Omega} |u_0(x, y) - c_1|^2 H(\phi(x, y)) dx dy \\ &\quad + \lambda_2 \int_{\Omega} |u_0(x, y) - c_1|^2 (1 - H(\phi(x, y))) dx dy. \end{aligned}$$

Let now

$$u = \begin{cases} \text{average}(u_0) \text{ inside } C, \\ \text{average}(u_0) \text{ outside } C. \end{cases}$$

Then,

$$u(x, y) = c_1 H(\phi(x, y)) + c_2 (1 - H(\phi(x, y))), \quad (x, y) \in \overline{\Omega}.$$

Fixing ϕ and minimizing $F(c_1, c_2, C)$ with respect to c_1 and c_2 , it is easy to express these constant functions of ϕ by

$$c_1(\phi) = \frac{\int_{\Omega} u_0(x, y) H(\phi(x, y)) dx dy}{\int_{\Omega} H(\phi(x, y)) dx dy} \quad \text{if } \int_{\Omega} H(\phi(x, y)) dx dy > 0,$$

$$c_2(\phi) = \frac{\int_{\Omega} u_0(x, y) (1 - H(\phi(x, y))) dx dy}{\int_{\Omega} (1 - H(\phi(x, y))) dx dy} \quad \text{if } \int_{\Omega} (1 - H(\phi(x, y))) dx dy > 0.$$

In the degenerate case $\int_{\Omega} H(\phi(x, y)) dx dy = \int_{\Omega} (1 - H(\phi(x, y))) dx dy = 0$, we obtain

$$\begin{cases} c_1(\phi) = \text{average}(u_0) \text{ in } \{\phi \geq 0\}, \\ c_2(\phi) = \text{average}(u_0) \text{ in } \{\phi < 0\}. \end{cases}$$

In order to compute the Euler-Lagrange equations, we use the variational level set approach and we arrive at

$$\frac{\partial \phi}{\partial t} = |\nabla \phi| [\mu k - \eta - \lambda_1(u_0 - c_1^2 + \lambda_2(u_0 - c_2)^2)], \quad \text{in } (0, +\infty) \times \Omega,$$

and $\phi(x, y, 0) = \phi_0(x, y)$ in Ω , where k is the curvature.

3. Numerical Experiments

In this section, we report on our numerical testing for the active contour algorithm without edges. By means of Example 1, basic properties of the algorithm are explained. The next example is a two dimensional medical image, in which we intend to segment parts of the spine. Finally, we apply the method to three-dimensional magnetic resonance data. Our numerical implementation is based on the MATLAB level set toolbox [MT05].

3.1. Example 1 (CMUC logo). For our first tests, we use the images shown in Figure 3, where the left image is the original image and the right one contains 10% of white Gaussian noise. Note that the left image in Figure 3 is not a binary image (i.e., it does not only contain black and white pixels), since the letters are drawn in different gray values. Both images have a resolution of 120×120 pixels. We use the working domain $\Omega = [-1, 1] \times [-1, 1]$, the parameters $\mu = 2$, $\lambda_1 = \lambda_2 = 1$ and the final time $t_f = 0.06$. This implies a mesh with mesh size $h = 1/60$ for the space discretization. We remark that, in [CV02] the scaling $h = 1$ is used, which results in $\Omega = [-60, 60]^2$ and in different scalings for the parameters $\mu, \lambda_1, \lambda_2$ and for Ω .

In Figure 4, the initial and final contours as well as seven intermediate steps of the time evolution for segmenting the CMUC logo with noise (Figure 3, left) are shown. As initial contour a circle is chosen, and as the time increases, this contour approaches the contour of the original image. Note that the topological changes needed to segment the different letters do not represent any problem for the algorithm.

Another attractive feature of the active contour algorithm without edges is that it also works in the presence of noise. This is essential when dealing with medical images, in which a certain amount of noise is unavoidable

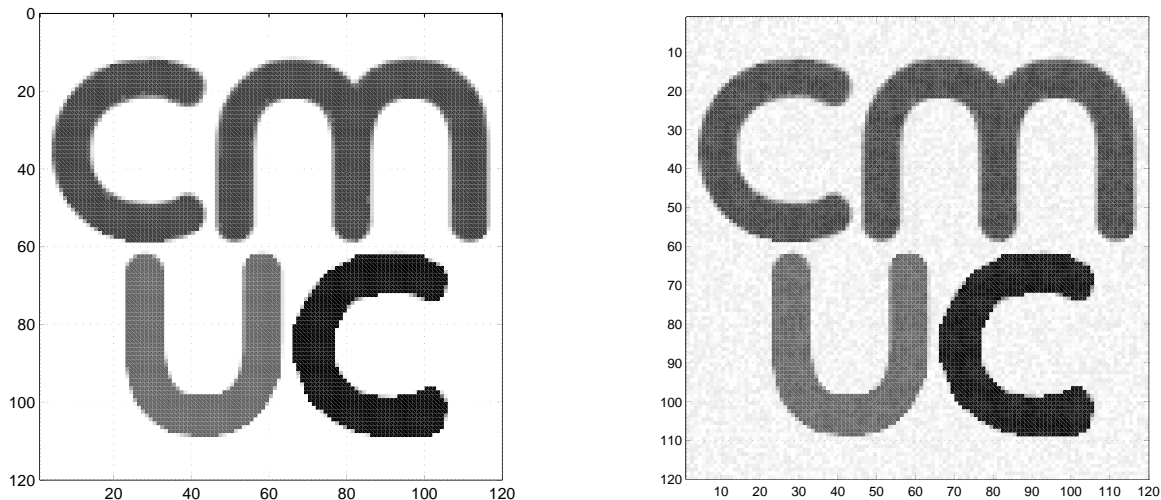


FIGURE 3. Example 1: Original image (left) and image containing 10% of white Gaussian noise (right).

due to background interferences or other perturbations. Our result obtained for the noisy image (Figure 3, right) can be seen in Figure 5. While noise presents a serious problem for segmentation algorithms that use image gradient information, the active contour method is stable with respect to noise in the image data and robustly detects the image contours.

3.2. Example 2 (2D medical image). In the second example, we attempt the segmentation of bones from the image shown on the left of Figure 6. We use the image domain $\Omega = [-1, 1] \times [-1, 1]$ and, for all tests, keep the parameters $\lambda_1 = \lambda_2 = 1$, $\nu = 0$ and the final time $t_f = 0.5$ fixed. We study the influence of μ , i.e., the weight for the term corresponding to motion in normal direction.

In the left of Figure 6 we show the evolution of the zero level set for $\mu = 0.1$. In the left plot of Figure 7, the resulting contour for this value of μ can be seen. In the middle and the right plot of Figure 7, the contour obtained with larger values of μ , namely $\mu = 0.3$ and $\mu = 0.5$ is shown. Obviously, the parameter μ allows to control the sensitivity of the contour in capturing details. Obviously, larger values of μ lead to smoother contours; these might

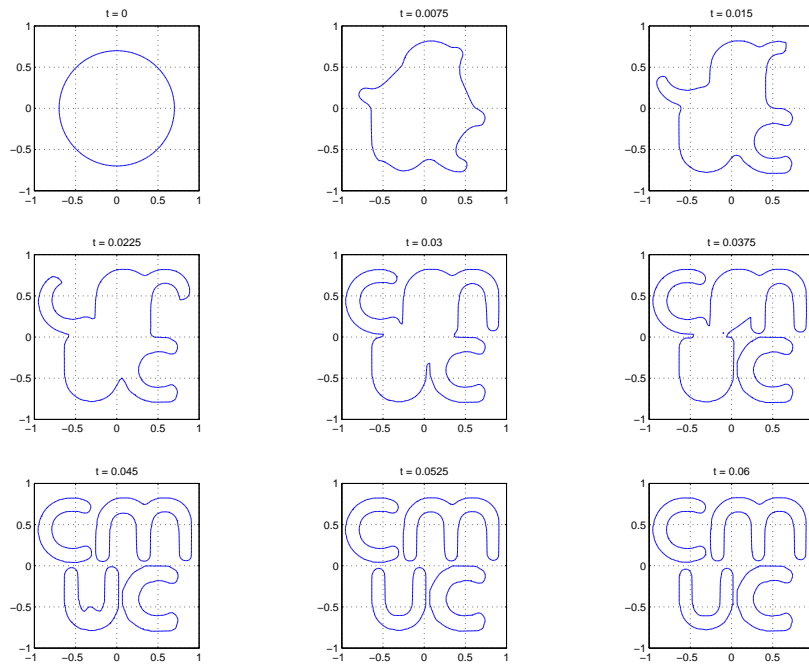


FIGURE 4. Example 1: Time evolution of level sets for the image shown on the left of Figure 3.

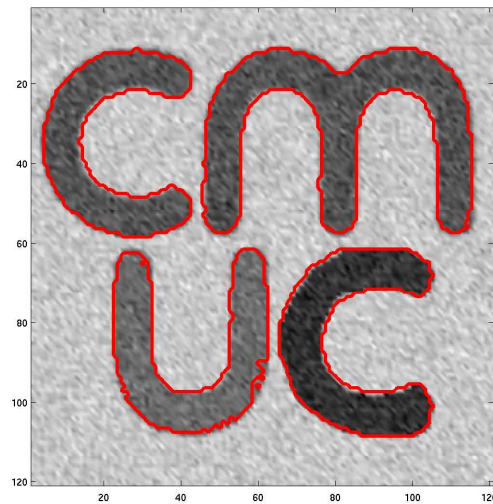


FIGURE 5. Example 1: Segmentation obtained for the noisy image shown on the right of Figure 3.

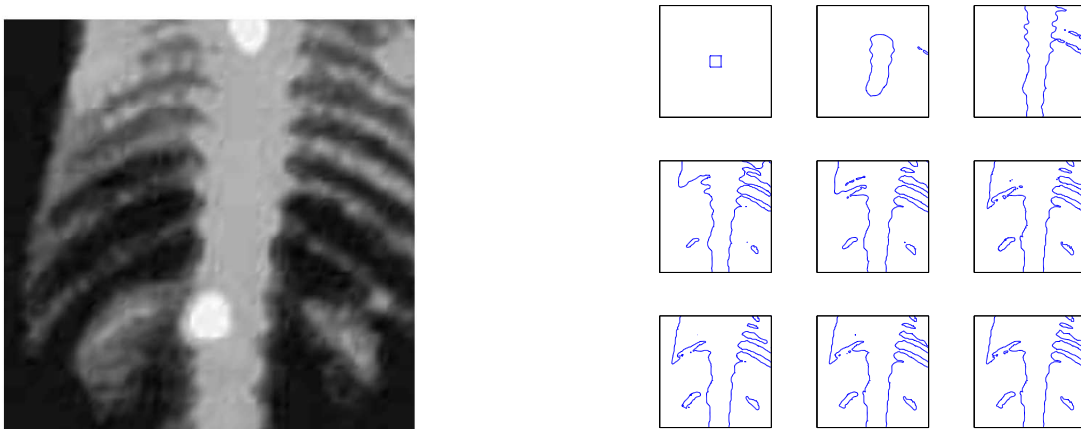


FIGURE 6. Example 2: Medical image (left) and level set evolution (right).

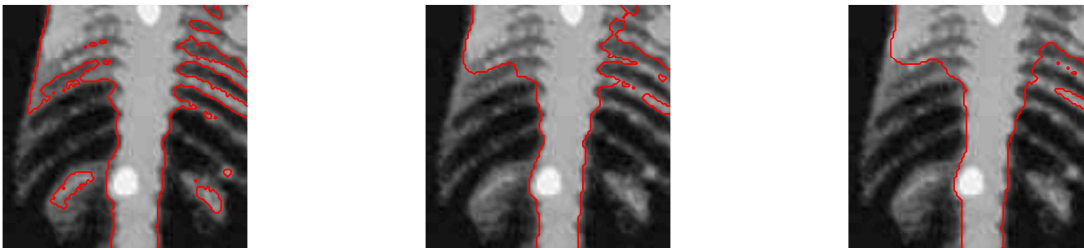


FIGURE 7. Example 2: Contour found using $\mu = 0.1$ (left), $\mu = 0.3$ (middle), and $\mu = 0.5$ (right).

be more stable with respect to noise in the image, but they possibly do not have the ability to find small structures.

3.3. Segmenting brain regions in 3D. The data for this problem is provided by the Institute of Biomedical Research in Light and Images of the University of Coimbra (IBILI). The idea is to identify the form of the putamen and caudate which are structures in the brain. The putamen is a portion of the basal ganglia. The basal ganglia system was associated with motor functions, as lesions of these areas would often result in disordered movement in humans (Chorea, athetosis, Parkinson's disease). If the PET scan shows decreased dopamine activity in the basal ganglia this aids in diagnosing Parkinson's disease.

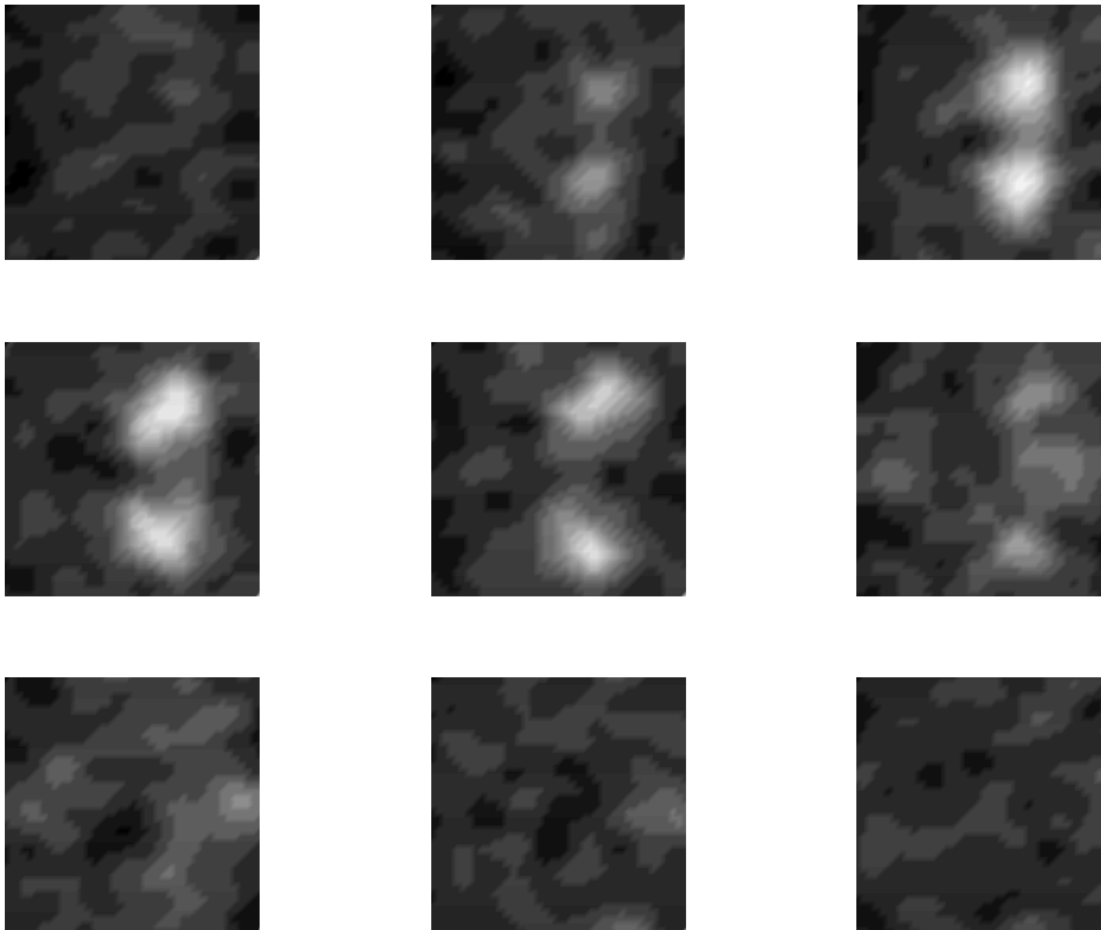


FIGURE 8. Example 3: Slices of magnetic resonance image.

We use a part of size $41 \times 41 \times 41$ of the original image. As before, the values of the data are between 0 and 255 and correspond to the gray values in the magnetic resonance image. We refer to Figure 8, where 9 two-dimensional slices of this data are shown. For our segmentation algorithm, we use the parameters $\lambda_1 = \lambda_2 = 1$, $\nu = 0$, $\mu = 0.05$ and the final time $t_f = 0.8$. As domain we choose $\Omega = [-1, 1]^3$ and as initial surface the cube $[-0.2, 0.2]^3$ is chosen. In our tests, we also used other initializations and obtained the same segmentation. However, if the initial zero level set was too small, it vanishes after the first steps of the iteration. The zero level sets for $\mu = 0.05$ at times $t = 0.0, 0.1, \dots, 0.8$ are shown in Figure 9. We compared the results for various values of μ and observed a similar behavior as for the two-dimensional examples: For $\mu = 0.001$, the solution captures more details of the data and the resulting surface is relatively rough (see the right plot in Figure 10).

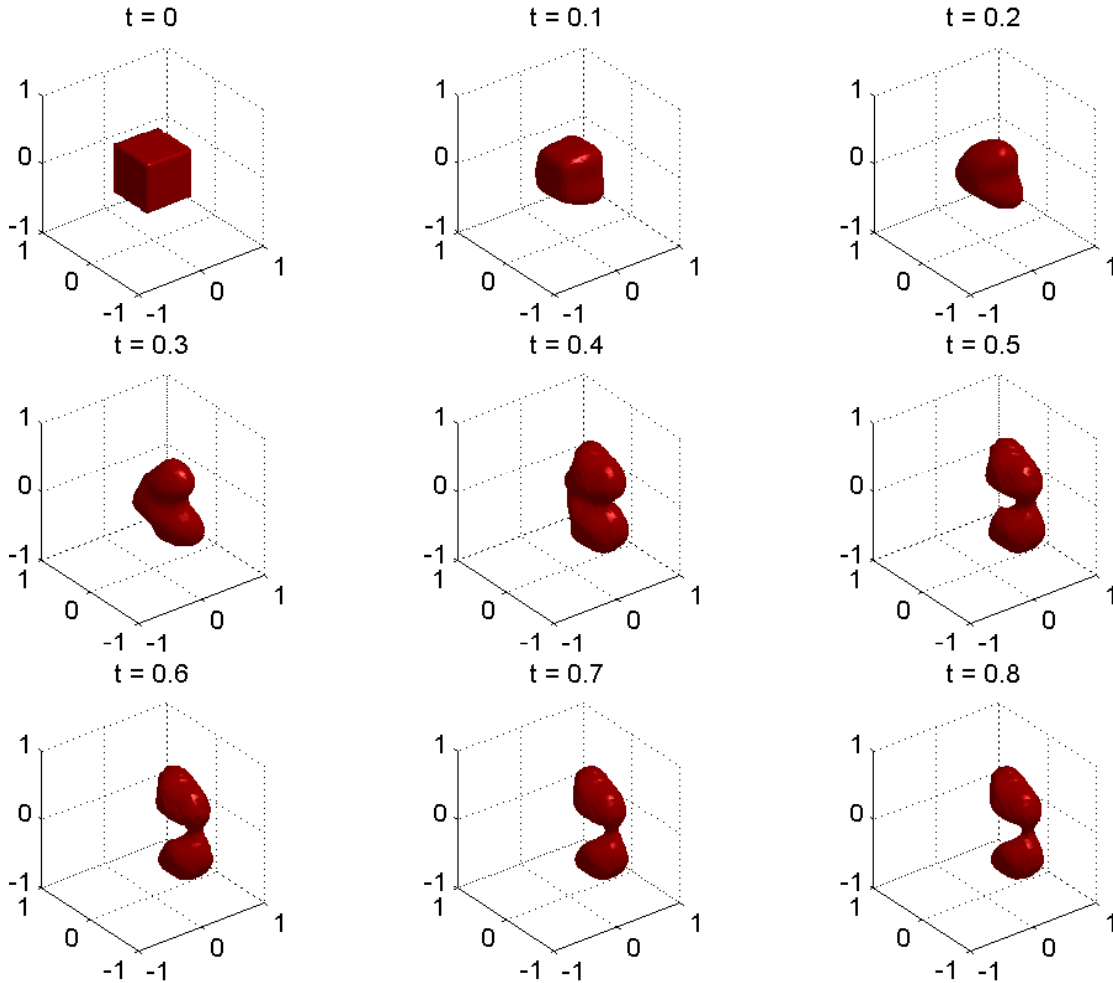


FIGURE 9. Example 3: Evolution of the zero level set in the iteration for $\mu = 0.05$.

For $\mu = 0.05$, the zero level set upon convergence is slightly smaller and smoother (see the left plot in Figure 10). For $\mu \geq 0.2$, independently from the initialization the zero level shrinks and finally vanishes. This undesired behavior happens if the weight μ for the term corresponding to motion in normal direction becomes too large.

4. Conclusions and further work

In this paper, we report on our numerical experiments with the active contour algorithm for image segmentation. Extensions of the present work interesting for doctors focus on the development of a low cost optical motion correction system for a SPECT/PET restraint free (without anesthesia) small

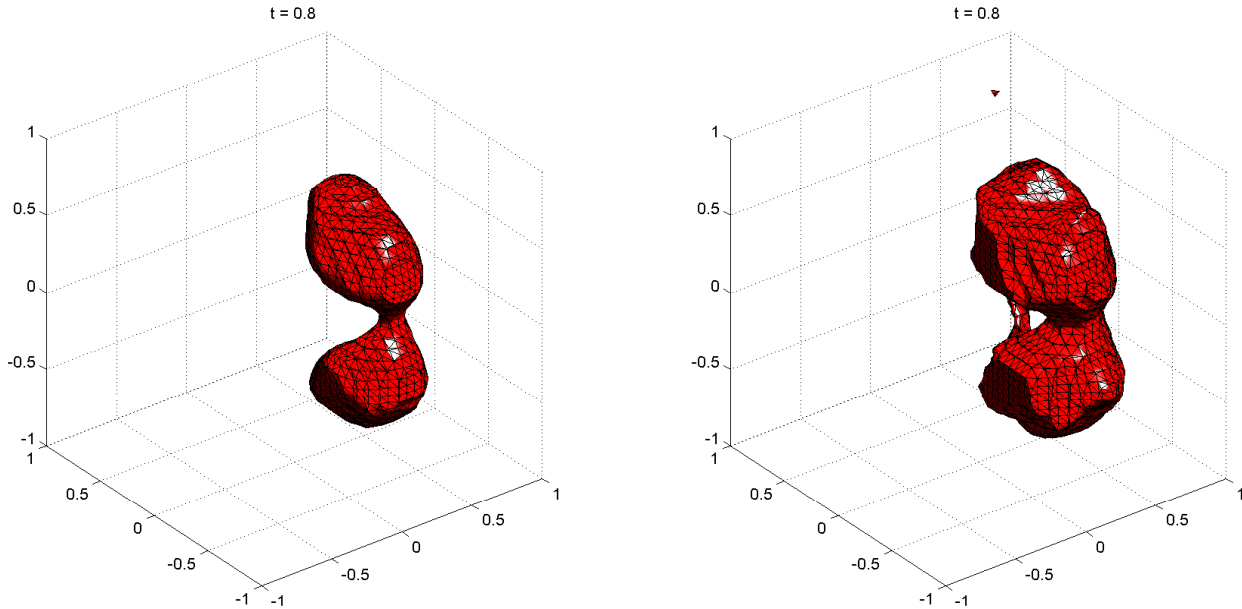


FIGURE 10. Example 3: Results of segmentation algorithm for $\mu = 0.05$ (left) and $\mu = 0.001$ (right).

animals. The problem of the implementation of this system can be divided in two major parts: motion detection and motion correction. One of the possibilities for using level sets in this context is to obtain the 4D contour (we must consider the time variable) of the animal.

References

- [CCCD93] V. Caselles, F. Catté, T. Coll, and F. Dibos. A geometric model for active contour in image processing. *Numer. Math.*, 66:1–31, 1993.
- [CV01] T. F. Chan and L. A. Vese. Active contour without edges. *IEEE Trans. Image Processing*, 10(2):266–277, 2001.
- [CV02] T. F. Chan and L. A. Vese. Active contour and segmentation models using geometric PDE’s for medical imaging. In *Geometric methods in bio-medical image processing*, Math. Vis., pages 63–75. Springer, Berlin, 2002.
- [MT05] I. M. Mitchell and J. A. Templeton. A toolbox of Hamilton-Jacobi solvers for analysis of nondeterministic continuous and hybrid systems. In *Lecture Notes in Computer Science (LNCS)*, volume 3414, pages 480–494. Springer Verlag, 2005.
- [OF03] S. Osher and R. Fedkiw. *Level set methods and dynamic implicit surfaces*, volume 153 of *Applied Mathematical Sciences*. Springer-Verlag, New York, 2003.
- [OS88] S. Osher and J. A. Sethian. Fronts propagating with curvature-dependent speed: algorithms based on Hamilton-Jacobi formulations. *J. Comput. Phys.*, 79(1):12–49, 1988.
- [Set99] J. A. Sethian. *Level set methods and fast marching methods*, volume 3 of *Cambridge Monographs on Applied and Computational Mathematics*. Cambridge University Press, Cambridge, second edition, 1999.

[ZCMO96] H. K. Zhao, T. Chan, B. Merriman, and S. Osher. A variational level set approach to multiphase motion. *J. Comput. Phys.*, 127:179–195, 1996.

A. ARAÚJO

CENTER FOR MATHEMATICS, UNIVERSITY OF COIMBRA, APARTADO 3008, 3001-454 COIMBRA, PORTUGAL

E-mail address: alma@mat.uc.pt

URL: <http://www.mat.uc.pt/~alma>

D. M. G. COMISSIÃO

CENTER FOR MATHEMATICS, UNIVERSITY OF COIMBRA, APARTADO 3008, 3001-454 COIMBRA, PORTUGAL

E-mail address: donna@mat.uc.pt

URL: <http://www.mat.uc.pt/~donna>

G. STADLER

CENTER FOR MATHEMATICS, UNIVERSITY OF COIMBRA, APARTADO 3008, 3001-454 COIMBRA, PORTUGAL

E-mail address: georgst@mat.uc.pt